



ISSN : 2347-2251

**Indo-American Journal of
Pharma and Bio Sciences**



www.iajpb.com

iajpb.editor@gmail.com
editor@iajpb.com

This article can be downloaded from
<http://www.iajpb.com/currentissue.php>



Power Flow Control of UIPC Using Neural Networks in AC-DC Grid Connected Hybrid Micro grids

Shaik.Kalesha1Mr.Ramesh2

1(M.Tech Student, Department of Electrical and Electronics Engineering, Quba College of Engineering AndTechnology, Venkatachalam,Nellore.A.P,India)

EMAILID:dsfkn.3ek228@gmail.com

2(Head Of The Department , Department of Electrical and Electronics Engineering, Quba College of EngineeringandTechnology,Venkatachalam,Nellore.A.P,INDIA)

EMAILID:ramesh.prams@gmail.com

Abstract:

Linking AC-DC microgrids in framework-related mixed microgrids may be improved by using a modified interphase power regulator, according to this study (UIPC). A normal matrix-related half-breed microgrid with an AC microgrid and a DC microgrid is the framework being studied. These microgrids are connected through a UIPC that has been modified rather than the same associated power converters. Change the current UIPC structure, which employs three force converters in each stage, to a reduced number of intensity converters for power trade control across AC-DC microgrids, the major goal of this work. Rather of having a power converter (LPC) for each stage, the redesigned structure use a bus power converter (BPC) to control the DC supply voltage. Because they can function in either capacitance mode (CM) or inductance mode (IN), LPCs, which feature DC transports, connect the AC microgrid to the main network (IM). A "fluffy rationale regulator" is utilized in the LPC control scheme. The H sifting process is used to broaden the fluffy derivation framework in order to eliminate errors in the development of enrollment capacity. Through the BPC, the DC microgrid distributes DC power to the LPCs. The LPCs' DC interface voltage changes in every circumstance since the DC microgrid power is supplied by a PV framework. Thus, another nonlinear unsettling influence onlooker (NDO-MS-SMC) approach for DC side management of the BPC is produced to settle the DC connect variances as a follow-up commitment to settle the DC connect variations Neural Networks are also used to assess the system's response.

A network controller replaces the current fuzzy controller. According to the simulation results, the enhanced UIPC's proposed power stream management method for mixed microgrids is a good fit.

I. INTRODUCTION

Since 2000, DC microgrids have been included into the conventional force

frameworks, including photovoltaic (PV) frameworks, energy units (FCs), vitality stockpiling frameworks (ESSs), and new DC loads, such as programmable DC electronic

burdens. As long as the AC power assets, such as wind turbines, and the AC loads are connected to the force frameworks through AC microgrids [2-3], they may be connected to the force frameworks. Microgrids that comprise both AC and DC power resources as well as commitments are referred to as half-breed microgrids [4]. Force converters connect the AC and DC microgrids. Using this agreement, the microgrids will be able to transfer power as necessary. As a result of this, force converters are often employed to increase intensity and maintain a consistent quality. Figure 1 depicts the usual structure of a matrix-associated half-breed microgrid. There may be PV frameworks, ESSs, and other DC transport-related loads in this diagram [6]. Typical AC microgrid components include a wind turbine, a diesel generator, and the AC loads that are often associated with AC transportation. [8] The force framework may either be coupled to the entire half and half microgrid or it can be removed. As shown in Fig. 1, the basic transports (joins) of two microgrids are linked by bidirectional

interlink power converter (ILCs) [9]. However, mimicking power converters in crossover microgrids has a number of specific issues, as follows:

Extreme voltage, stage, recurrence, and force change are only a few of the distinctive features of microgrids.

Many microgrids may be used to create a mixing microgrid. For example, there may be three microgrids: two AC and one DC. Because the voltage magnitude and period of

the basic transports of the microgrids must be identical in order to prevent current flowing between equal related ILCs, such a configuration is challenging and puzzling.

ILCs within a microgrid must have equivalent force evaluations to ensure that the transferred force is distributed evenly.

There are a number of factors that may effect how the equal-related ILCs perform when it comes to sharing power.

When there is a problem with one ILC, the deficient current may be divided unevenly across the ILCs because of the nonlinear nature of the issue. If the force converters' specified current constraints are exceeded, the force converter will be disconnected, resulting in a significant loss in transferred power. As a consequence, a microgrid may have load concealment or even precariousness.

The intermittent behavior of some distributed generation (DG) units in microgrids causes a lot of uncertainty in generated power and oscillations in traded power across microgrids. -

harmonics may generate a phase mismatch between ILCs, which results in voltage loss in an AC microgrid [15].

Parallel-connected ILCs may be powered by a variety of different types of electricity. Power sharing performance suffers as a consequence of voltage and power variations..

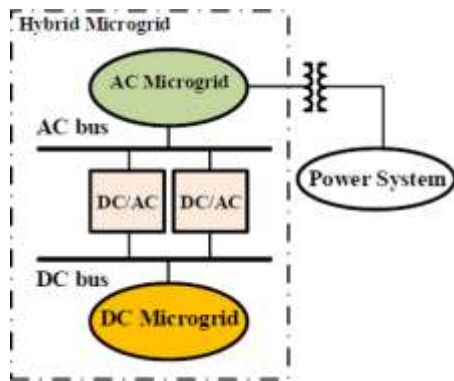


Fig1A typical grid-connected hybrid microgrid

It has been suggested in writing that various procedures and control tactics may be used to deal with the issues listed above. For ILCs with equal coupling in both directions, [12] suggests a new leveling control technique. Fixed reference outline (SRF) and consonant review were the foundations of the control method, which had no uniform word throughout the tomahawks. This strategy has a lot of benefit since it's simple to apply because to the SRF organization. [13] described a multiple-tiered control system based on hang control, with a hang plot serving as the primary control level. On the DC side, the proportionalresonant (PR) regulator was built, while the corresponding essential (PI) regulators were used. In order to link the crossover microgrid to the utility, the third control level exploited the wave created as a consequence of the main level control activity. A flaw-protected dynamic force control system for network-connected crossover microgrids has been reported in [14]. The method employed a customizable scalar to distinguish between dynamic and receptive force movement magnitudes. Force vacillation is caused by a voltage imbalance, as proven in [15]. Parallel-connected ILCs may be controlled using a new technique in which each force converter's current is managed to change the overall flow of all ILCs. With this new designation as "excess," one ILC obtained

better scores than the rest of the group. A expensive control strategy is as a consequence.

Consonant bending renders the proposed solution ineffective, as does its inability to limit reaction force motions. A robust control plot was used in [16] to regulate power sharing between two equal related inverters. The method has been used to build the present regulator of unions through union examination.

inverters. [17] proposes an optimum fragmented request regulator for power sharing between two parallelconnected inverters. The scientists in [18] have designed cross breed microgrids in accordance with IEEE 1547.4-2011. [19] depicts a decentralized and self-advanced control structure for restricted microgrids. The control strategy has provided neighborhood control activities with no correspondence connections, resulting in a more solid strategy. The FACTS (Flexible AC Transmission System) devices have also been used to manage power flow in AC transmission systems. In this article, UIPC is used to manage the traded power across microgrids as well as serve as a basic foundation in a cross breed microgrid. The Realities devices have been used in a variety of force control applications with different control topologies. The binding together force stream regulator (UPFC) was used to improve

voltage stability in [20]. Hereditary calculations have also been used to determine the optimal fraction of UPFCs. [21] used the between line power stream regulator (IPFC) to regulate the moving force in a transmission line to perfection. The static VAR compensators (SVCs) were implemented by the designers in [22] to strengthen the force framework security using monetary research. In a transmission line that connects two territories in a force framework, the static

In a mixed microgrid situation, this article focuses on a small scaled changed UIPC to govern the traded power across microgrids as a principal network. The following are the main commitments of this project:

The UIPC is suggested to regulate the traded power across microgrids as well as the basic network in a half and half microgrid, rather of using equal associated power converters, which have several control concerns [8-17]. The standard UIPC structure, which uses three force converters in each stage, has been modified to use a smaller number of intensity converters for power exchange control across AC-DC microgrids. - Because the microgrid elements in a cross breed microgrid are not quite the same as the ordinary force framework elements, controlling the UIPC with a DC microgrid associated with its DC transport would be a difficult task, which is addressed in this work, and another NDO-MS-SMC-based control technique for the DC side control of the BPC is introduced. As a result, the focus of this study is on using the UIPC as an optional solution for power stream management across many microgrids in half and half microgrids.

Unlike standard equal associated power converters, the UIPC has the following advantages: - Control of traded power across microgrids without imposing burdensome

simultaneous arrangement compensator (SSSC) has been used [23]. The SSSC has shown to be effective when it comes to trading power control between two areas. The UIPC was introduced for the first time in [24]. It's an improved version of the traditional IPC (interphase power regulator), using force converters in place of stage moving transformers in each stage. The UIPC's suitability for power stream regulation has been shown in [24].

constraints, such as identical voltage extents, stages, and so on, which are often required to connect ILCs in an equal manner.

- The UIPC, as shown in [24], may unquestionably limit the defect current without the requirement for an excess force converter, as shown in [15]. In comparison to control approaches such as the fast force control plot, which has traditionally been used for equal related ILCs, this aspect makes the interconnection more trustworthy, affordable, and less complex.

- Despite equal related ILCs allowing for direct electrical connections across microgrids, the proposed altered UIPC allows for voltage confinement, as demonstrated in [24].

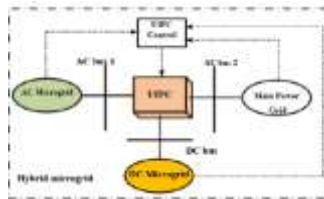
- The UIPC can manage the DC transport voltage of a DC microgrid in the same way as it can control the AC transport voltage of an AC microgrid. The usual equal related ILCs were not used to create this trademark.

In this study, a modified variation of the UIPC is used to link half and half microgrids, achieving all of the previously described benefits. The rest of the work is organized as follows: The revised UIPC is shown in Section II. Segment III shows how to discover the vacillations of the usual DC

transport voltage of the changed UIPC using another

aggravation eyewitness based powerful multiple surface sliding mode control approach. Section IV provides the reproduction results as well as correlation contextual evaluations. Finally, Section V follows the completion of the assignment.

PROPOSED UIPC BASED STRUCTURE OF HYBRID MICRO GRID AND DYNAMIC



MODELING

II. The proposed hybrid microgrid topology for the UIPC is described in this section. This part also includes the dynamic model of the improved UIPC. The hybrid microgrid under investigation is shown on Figure 2. One AC microgrid and one DC microgrid are linked via the UIPC in the grid-connected hybrid microgrid, as depicted. A diesel generator and associated AC and DC loads make up the AC microgrid. The DC microgrid includes a PV system, a battery, and AC and DC loads. The common DC bus connects the loads, the PV system, and the batteries (DC link).

Figure 2: UIPC-based interconnection of AC-DC microgrids in a grid-connected hybrid microgrid.

A. Traditional UIPC

[24] describes the UIPC's per-phase model, which is seen in Fig. 3. The phase-moving transformers of the interphase power regulator (IPC) were replaced with voltage source converters in this arrangement (VSCs). In each stage, two AC transports, such as..1 and..2, are Lines j1, 2, and 3 are to be found. Transformers Tj pump the series voltage $V_{sese} = V_{ser} + jV_{sei}$ into each line via these converters.

V_{ser} and V_{sei} are the real and imaginary components of the injected series voltage. The impedance of a line is given by $ZL_j = RL_j + jXL_j$. A voltage source managed in this manner is most often used as the injected series voltage source:

K_A and K_P stand for the amplitude and phase coefficients, respectively, of a voltage signal. With the

linked by three VSCs, such as VSC1, VSC2, and VSC3. VSC1 and VSC2 are stage-moving converters, but VSC3 is a voltage-controlling converter. VSC1 operates inductively, infusing the arrangement voltage.

T1 connects the line to the transformer. VSC2, on the other hand, operates in capacitive mode, infusing the arrangement voltage..... to the line through transformer T2. The third VSC, for example VSC3, is connected to one of the AC transports, in this case..1, through transformer T3 and regulates the AC voltage. All of the VSCs have the same DC transport, which is supplied by a constant capacitor. In this way, the DC connect voltage..... is responsible for each VSC's dynamic forces. As a result, the exchanged power between the two AC transports would be regulated by stage edge control of VSC1 and VSC2. [24] has more nuanced information.

For example, in Figure 3, the UIPC contains three power converters in each phase. [24]

B. The suggested structure of the UIPC

It will begin by changing the UIPC's conventional topology, as mentioned in the previous paragraph. In the next part, we'll discuss the UIPC's new control method. Fig. 3 shows the UIPC's conventional structure, which is riddled with problems: Connecting three phases of AC buses needs nine VCSs and nine power transformers due to the usage of three VSCs in each phase, making the system exceedingly costly.

- The DC connections of all VSCs in each phase are connected in parallel. There is a tendency for the common DC link voltage to oscillate if the output power of VSCs fluctuates or if a disturbance occurs in the system model, such as a change in the system parameter [12, 25]. VSCs with a shared DC connection have a major difficulty with voltage fluctuation in the DC link. In [24], this issue was not addressed.

According to the modified UIPC model (Fig. 4), these impediments may be eliminated. Only one power converter, LPC_j , is used in each phase, as stated.

phase coefficient K_P equal to 1 and se usually equal to 2, the voltage amplitude coefficient K_A is a function of the pulse width modulation (PWM) technique. The injected voltage phase angle would be used to synchronize the anti-parallel thyristor switches S1 and S2 in the control system. Only one of these switches is active at any one moment, depending on the phase angle sign. When the voltage phase coefficient K_P is equal to +1 and S1 is on and S2 is off, the UIPC is in inductive mode (IM). It follows that the phase coefficient is also a factor in this case.

In capacitive mode (CM), the UIPC is turned off and S1

$$\begin{aligned}\varphi_{se}^L &= \varphi_1 + \alpha_1 \\ \varphi_{se}^C &= \varphi_2 + \alpha_2\end{aligned}$$

is switched on, while KP is -1. This means that both AC buses V1 and V2 may be adjusted in terms of power transmission. Figure 4 further shows that there is only

$$\begin{aligned}V_1 \angle \delta_1 - V_2 \angle \delta_2 &= (R_{L1} + jX_{L1})I + V_{se} \angle \varphi_{se} \\ &= (R_{L1} + jX_{L1}) \frac{P-jQ}{V_2^r - jV_2^i} + (V_{se}^r + jV_{se}^i) \\ &= \left(\frac{V_2^r (R_{L1}P + X_{L1}Q) + (X_{L1}P - R_{L1}Q)}{(V_2^r)^2 + (V_2^i)^2} + V_{se}^r \right) \\ &\quad + j \left(\frac{V_2^r (X_{L1}P - R_{L1}Q) + (R_{L1}P + X_{L1}Q)}{(V_2^r)^2 + (V_2^i)^2} + V_{se}^i \right)\end{aligned}\quad (9)$$

one BPC for each step of the process. The BPC's DC bus is then connected to the DC microgrid. V1 of the AC microgrid bus is also connected to the BPC, which manages the AC voltage and facilitates power exchange with the DC microgrid through a transformer TBPC, as shown in the figure. In Fig. 5, the suggested UIPC's injected voltage is shown in the system voltages. This graphic provides the following information.:

The power balancing equation may be used to calculate the transferred power between the DC and AC links (..1):

where IDCUIPC is the current flowing in the UIPC's DC link, and V1d and i1d are the AC link's d-axis voltage and current, respectively

$$V_{se} = K_A V_{DC} \angle K_P \varphi_{se}$$

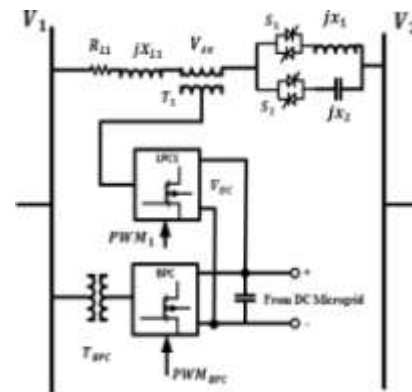
The UIPC's different working modes, such as $P = \frac{R_{L1} V_1 V_2 (\cos \delta_1 \cos \delta_2 + \sin \delta_1 \sin \delta_2 + R_{L1} V_2^2) - X_{L1} V_1 V_2 (\cos \delta_1 \sin \delta_2 - \sin \delta_1 \cos \delta_2)}{R_{L1}^2 + X_{L1}^2}$ (5)

CM, are taken into consideration while calculating the phase angle of the voltage at the receiving end $Q = \frac{R_{L1} V_1 V_2 (\cos \delta_1 \sin \delta_2 - \sin \delta_1 \cos \delta_2) + X_{L1} V_1 V_2 (\cos \delta_1 \cos \delta_2 + \sin \delta_1 \sin \delta_2 + X_{L1} V_2^2)}{R_{L1}^2 + X_{L1}^2}$ (6)

Equations (2) and ((3)).3).

According to the sophisticated power flow paradigm [26], the transmitted power between the two AC buses would be estimated as follows.:

The voltages V1 and V2 have phase angles of 1 and 2, respectively. After some math manipulations, Equation (4) can be written as follows:



In microgrids, $RL1 \gg XL1$ and we get:

So, the active power is controlled by how high the voltages are on the AC buses, and the reactive power is controlled by how far apart the phases are. The proposed UIPC controls the magnitude and phase angle difference of the voltage. This means that the active and reactive powers that are exchanged between two AC buses can be easily controlled. Using the Kirchhoff Voltage Law and Fig. 6, we can figure out what will happen when a voltage is injected of the UIPC:

In the microgrids, $XL1P \cong RL1Q$ and we get:

$$S = V_2 \left(\frac{V_1 - V_2}{Z_L} \right)^* = \frac{(V_1 \cos \delta_1 + jV_1 \sin \delta_1 - V_2 \cos \delta_2 - jV_2 \sin \delta_2)^*}{R_{L1} - jX_{L1}} \quad (4)$$

Also, $RL1P \gg XL1Q$ and we have:

Figure 4 shows the proposed UIPC topology (each phase implements only one power converter, named as LPC)

Fig.5.VoltageswhentheproposedUIPCisinvolved

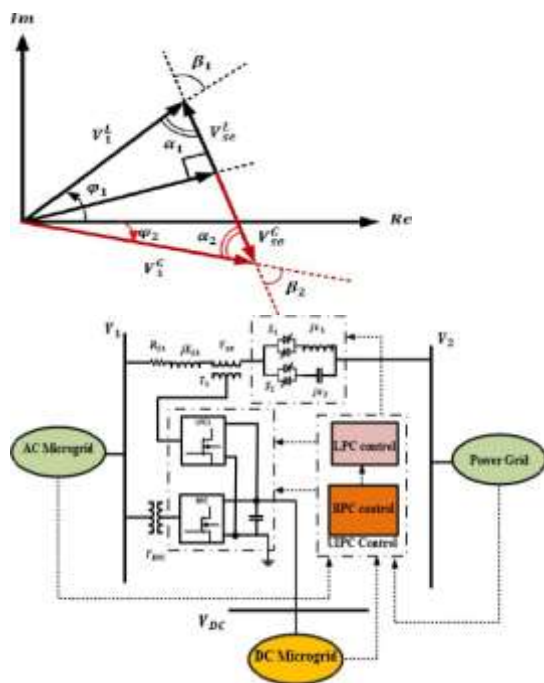
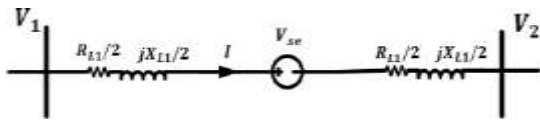


Figure 7: A per-phase model of AC-DC microgrid connectivity utilizing the UIPC and its control system.

Immediately, in contrast to the traditional structure, The following benefits come from the suggested UIPC geography:

- Each step only needs a single LPC.
- Only one BPC is needed for the three-stage configuration. So, the general model needs to use four voltage source converters (VSCs) and three force transformers.

Figure 6 shows a model of each phase of the system with the proposed UIPC's injected voltage.

Figure 7 depicts the per-stage geography of the proposed UIPC-based linked microgrids in the cross breed microgrid. The planned UIPC's overall control structure is also shown in this diagram. There are two subsystems in the control framework: series VSC control and NDO-MS-SMC based DC connect control. The Series VSC Control subsystem regulates the injected voltage and switches S1 and S2, and its construction employs an ideal H based fluffy logic regulator. The next subsection depicts the control subsystem. The SMC-based DC connect Control subsystem is responsible for balancing out regular DC interface voltage vacillations and is dependent on a hearty different surface sliding mode control system that is based on aggravation spectators. The following section depicts this control structure method.

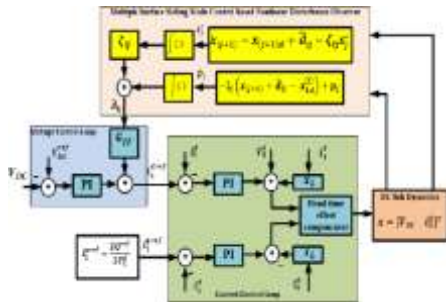
- The DC interface voltage is given by the DC microgrid. This part is used by the UIPC to connect the AC and DC microgrids.

- An ideal fuzzy reasoning regulator is used in the control structure of LPCs, which cuts down on mistakes.

A. Proposed plan for controlling LPC

Figure 7 shows the suggested control plot for the proposed UIPC structure. It has two control subsystems: a control scheme for the LPC and a control plot for the BPC based on the SMC. There are also control cooperations in these subsystems of control. Fig. 8 shows

the control method that is suggested for each LPC at each step. As far as I can tell, the voltage and line current of the infused arrangement are calculated and scaled. The important parts of these scaled signs are then taken out



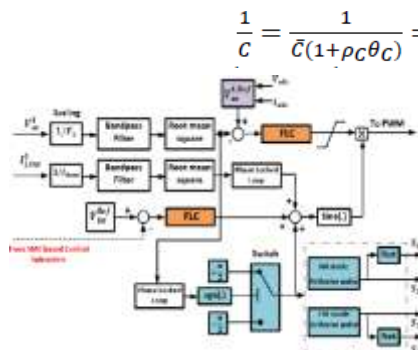
with a bandpass channel. MATLAB [27] is used to solve the channel's limits (move work) in the following way:

- The DC interface's voltage changes are smoothed out by a technology called "variable surface sliding mode control" and an effect called "uncomfortable influence." This will be shown in the next section.

The root mean square (rms) values of the signals that have been filtered are then found. The injected voltage error is used to find the best fuzzy logic controller (FLC). A PLL is used to figure out the phase of the voltage that is injected. Then there's the symbol for the phase., This sign, which is really KP in Equation (1), is found, and based on this sign, it is assumed that the UIPC works in either IM or CM mode. So, the right phase shift is used,

$$\begin{cases} \frac{dV_{DC}}{dt} = -\frac{3V_1^d i_1^d}{2CV_{DC}} + \frac{1}{C} I_{dist} \\ \frac{di_1^d}{dt} = \frac{V_0^d - V_1^d}{L} - \omega i_1^q - \frac{R}{L} i_1^d \end{cases}$$

which is +2 for IM mode and 2 for CM mode. Also, the switches S1 and S2 are turned on or off depending on the mode of operation. The H filtering design method, which has been fully explained and confirmed by the authors of this paper in [28], is used to make the ideal FLC. As shown in Fig. 8, a DC link voltage



$$\frac{1}{c} = \frac{1}{\bar{c}(1+\rho_C\theta_C)} = \frac{1}{\bar{c}} - \frac{\rho_C}{\bar{c}} \theta_C (1 + \rho_C\theta_C)^{-1}$$

In reality, as previously stated, the BPC is in charge of regulating the DC connection, therefore the suggested NDO-MS-SMC method is applied to the DC link.

compensation unit. To catch up on the constitutional delay nested in the dynamics of the current control loop and the suggested disturbance observer, the voltage control loop utilizes optimum proportional-integral (PI) controllers accompanied by the feedforward power disturbance. The evolutionary algorithm is used to optimize the PI controllers in both current and voltage control loops (GA).

Figure 9: A novel NDO-MS-SMC technique is used to control the BPC's DC link.

B. Nominal system dynamic model

To begin, the nominal model will be used to derive the dynamic equations of BPC's common DC connection without applying any parametric uncertainty. We obtain the following using Kirchhoff Current Law:

It's the angular frequency, expressed in rad/s, that's used, and the output filter inductance and resistance are V_0 and V_1 (the AC bus to which the BPC is connected), respectively..

As a result of Equations (12), (14) and (15), we get:

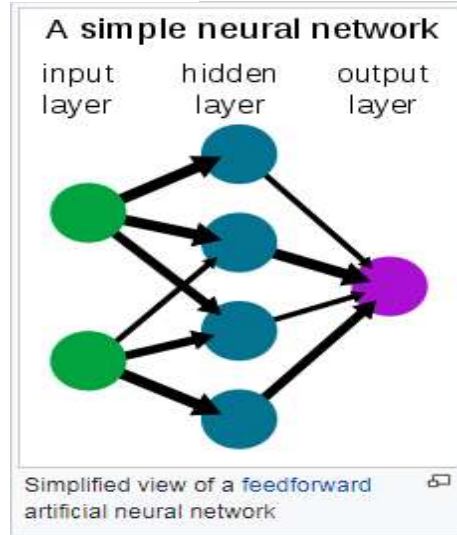
A system with nonlinear terms is shown by equation (17). This is the system's nominal model.

C. A perturbed system dynamical model

The following are the uncertainties for the DC link Inductance L and capacitance C should be rebuilt using the following disturbance parameters::

$$d_1(x, t) = \frac{\bar{I}_{dist}}{\bar{C}} + \left(\frac{3V_1^d x_2}{2x_1} \right) \rho_C \theta_C (1 + \rho_C \theta_C)^{-1} + \frac{\bar{I}_{dist}}{\bar{C}} \rho_{I_{dist}} \theta_{I_{dist}} - \frac{\bar{I}_{dist}}{\bar{C}} \rho_C \theta_C (1 + \rho_C \theta_C)^{-1} (1 + \rho_{I_{dist}} \theta_{I_{dist}}) \quad (23)$$

$$d_2(x, u, t) = -\omega i_1^q + \frac{\rho_L \theta_L}{\bar{L}} (R x_2 - u + V_1^d) (1 + \rho_L \theta_L)^{-1} \quad (24)$$



To use nonlinear control terminology, we refer to the uncertainty in $d_1(x,t)$ as "matched" and the uncertainty in $d_2(x,u,t)$ as the "unmatched". That's why this is how it's generally done now:

where, $b=1L$. The disturbance in (25) is continuous

Step 2. Define the multiple surfaces sliding surfaces, as follows [30]:

$$\frac{1}{L} = \frac{1}{\bar{L}(1 + \rho_L \theta_L)} = \frac{1}{\bar{L}} - \frac{\rho_L}{\bar{L}} \theta_L (1 + \rho_L \theta_L)^{-1}$$

(20)

(18)

(19)

where x_{jd} is a positive constant representing the intended state trajectory. Each sliding surface s_j must be set to zero such that $x_j x_{jd}$ is equal to zero. Our first sliding surface

$$\begin{aligned} \dot{x}_1 &= \left(\frac{1}{\bar{C}} - \frac{\rho_C}{\bar{C}} \theta_C (1 + \rho_C \theta_C)^{-1} \right) \left(-\frac{3V_1^d x_2}{2x_1} \right) \\ &+ \left(\frac{1}{\bar{C}} - \frac{\rho_C}{\bar{C}} \theta_C (1 + \rho_C \theta_C)^{-1} \right) \left(\bar{I}_{dist} (1 + \rho_{I_{dist}} \theta_{I_{dist}}) \right) \\ &= -\frac{3V_1^d x_2}{2\bar{C}x_1} + \frac{\bar{I}_{dist}}{\bar{C}} + \left(\frac{3V_1^d x_2}{2x_1} \right) \rho_C \theta_C (1 + \rho_C \theta_C)^{-1} + \\ &\frac{\bar{I}_{dist}}{\bar{C}} \rho_{I_{dist}} \theta_{I_{dist}} - \frac{\bar{I}_{dist}}{\bar{C}} \rho_C \theta_C (1 + \rho_C \theta_C)^{-1} (1 + \rho_{I_{dist}} \theta_{I_{dist}}) \end{aligned} \quad (21)$$

$$\begin{aligned} \dot{x}_2 &= \left(\frac{1}{\bar{L}} - \frac{\rho_L}{\bar{L}} \theta_L (1 + \rho_L \theta_L)^{-1} \right) (-R x_2 + u - V_1^d) - \omega i_1^q \\ &= \frac{R}{\bar{L}} x_2 + \frac{u}{\bar{L}} - \frac{V_1^d}{\bar{L}} - \omega i_1^q + \frac{\rho_L \theta_L}{\bar{L}} (R x_2 - u + V_1^d) (1 + \rho_L \theta_L)^{-1} \end{aligned} \quad (22)$$

Artificial intelligence:

Faux neurons, also known as artificial neural networks (ANN) or imitated neural networks (SNN), are networks of normal or artificial neurons that utilize scientific or computational models for data processing that are based on the connectionistic technique of calculation. As information flows in and out of a system, an ANN's internal structure adapts to accommodate these changes.

If you want to put it another way: Neural systems, or dynamic instruments, are non-linear presentations of factual information. In addition to finding patterns in data, they may be used to highlight complex connections between data sources and outputs. Using simple preparation components (fake neurons), a counterfeit neural system is able to display a wide range of global behavior that is governed by the interactions between component boundaries and component handlers themselves. When Warren McCulloch and Walter Pitts first exhibited fake neurons at the University of Chicago in 1943, they were both neurophysiologists and rationalists.

There are other terms used to describe a network of neurons that is based on the connectionistic technique of

downloaded from
/currentissue.php

calculation, such as "fake neural system," "artificial neural system," and "simulated neural system." It is common for an artificial neural network (ANN) to change its structure in reaction to external or internal input.

Neural systems, to put it another way, are non-linear presentations of factual information or dynamic instruments that are non-linear. Additionally, they are a useful tool for discovering patterns in large amounts of data.

To create a fake neural system, you'll need a few fundamental preparatory components (fake neurons), and they may show a wide range of global behavior depending on how they're linked together. In 1943, neurophysiologist Warren McCulloch and rationalist Walter Pitts presented the first fake neurons at the University of Chicago.

The repeated Hopfield arrangement is an example of an older kind of counterfeit neural system

There is some evidence that Alan Turing first introduced the idea of a neural system as "B-type chaotic machines" in his 1948 book *Intelligent Machinery*. The effectiveness of fake neural system models stems from their ability to receive and utilize information from senses. The Boltzmann machine (1983) and, more recently, deep learning calculations, which can verifiably gain proficiency with the observed information's dissemination capacity, can both be used by unaided neural systems to learn information representations that capture the unique qualities of information appropriation. The use of neural networks for learning is especially advantageous when it is hard to prepare skills manually due to the unpredictable nature of the material or assignment.

Applications:

A broad variety of applications benefit from neural systems. On errands that fall into one of the following categories, the employment of fake neural networks is common.

Relapse evaluation, including time estimation and presentation of function.

A sequential dynamic and recognition of instances and groups, as well as an acknowledgment of novelty.

Sorting and grouping, as well as dazzling signal splitting and pressure balancing

Some of the applications of ANN include nonlinear framework identification and control (vehicle control, process control), game-playing and dynamic (backgammon, chess, dashing), design acknowledgment (radar frameworks, face ID, object recognition), grouping acknowledgment (motion, discourse, transcribed content acknowledgment), clinical conclusion and monetary applications, as well as information mining (or information revelation in databases), "KDD," and perception and email. Semantic profiling of a client's preferences based on photos produced for object identification may be done, for example. Some of the applications of ANN include nonlinear framework identification and control (vehicle control, process control), game-playing and dynamic (backgammon, chess, dashing), design acknowledgment (radar frameworks, face ID, object recognition), grouping acknowledgment (motion, discourse, transcribed content acknowledgment), clinical conclusion and monetary applications, as well as information mining (or information revelation in databases), "KDD," and perception and email. Semantic profiling of a client's preferences based on photos produced for object identification may be done, for example.

Neuroscience:

Hypothetical and computational neuroscience is concerned with examining natural brain frameworks in a hypothetical manner and exhibiting the results in a computational manner. It's because neuronal frameworks are linked to a person's mental processes

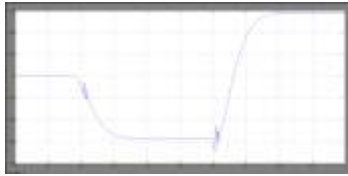
The field's concentration is on psychological and social display.

To get a better understanding of how natural brain frameworks function, scientists are working to build artificial ones. The only thing neuroscientists are aiming for is an organically conceivable instrument for neuronal handling and learning (organic neural system models) and hypotheses (factual learning hypothesis and data hypothesis).

Types of models

Each model has a different amount of consideration and presents a distinct piece of the neural system. neurons' transient conduct models, from models of the hardware formed by cooperation between neurons, to models of conduct coming from conceptual brain modules that talk to full subsystems. Both the neuronal structure itself as well as its link to learning and memory have been studied in regard to these concepts of neural framework pliability.

SIMULATION RESULTS:



DcLINK VOLTAGE

Fig. 14. Active power of DC link when 40 kW is demanded from the AC side

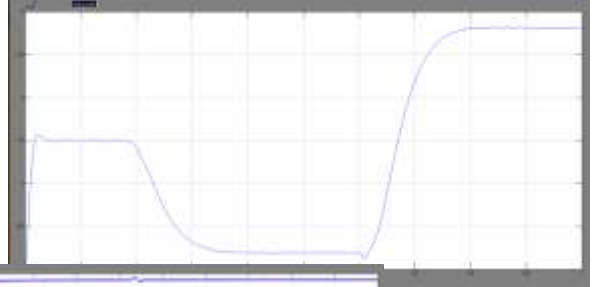
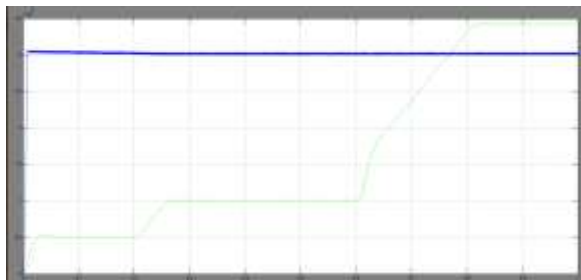


Fig.13.Generation in each micro grid

CONCLUSION:



Pse Injected Power

DcLINK VOLTAGE

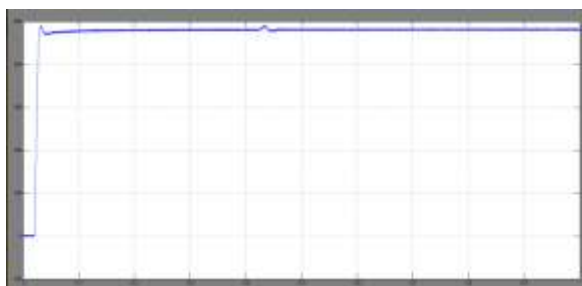
Fig. 14. Active power of DC link when 40 kW is demanded from the AC side



The hybrid microgrid structure is the most probable option in the future smart grid to gather together the

both AC and DC loads may be powered by renewable energy resources. Thus, the benefits of AC and DC microgrids may be combined in this system. Regulating the flow of electricity between interconnected AC and DC microgrids is a common challenge in this design. In this study, a UIPC-based technology was used to give an alternative to parallel-connected power converters. New and improved control methods have been established for the UIPC after its restructuring. Simulated results showed that both the enhanced model and its capacity to manage the power exchange between AC and DC microgrids were accurate. Fuzzy logic is outperformed by the neural network controller.

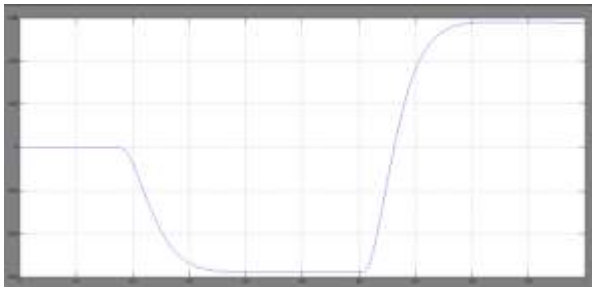
Referrals are included in this section.



d from sue.php

When it comes to DC microgrids, Runfan Zhang and Branislav Hredzak published an early-access work in IEEE Transactions on Smart Grid in 2018.

IEEE Transactions on Smart Grid, Vol. 5, No. 4, 2014, p.



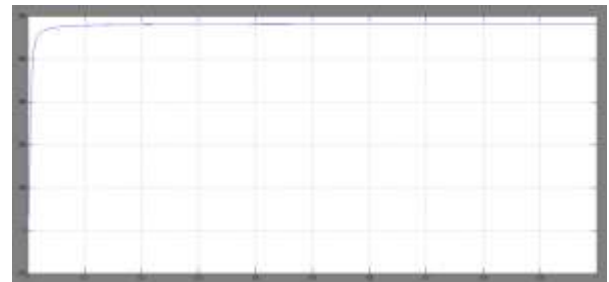
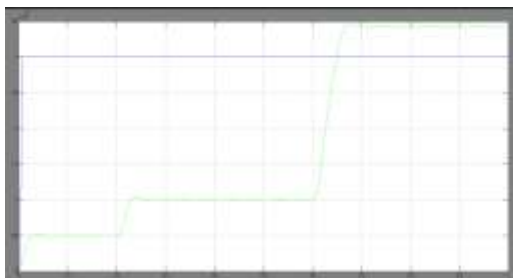
Study on Robust Control of Microgrid Energy Storage Systems Using Various Approaches, IEEE Trans. on Smart Grid, Jongwoo Choi et al., Early Access, 2018.

Distributed Model-predictive Real-time Optimal Operation of a Network of Smart Microgrids, Early Access, 2018, by IEE Smart Grid Transactions

VSESeriesInjectedVoltage

For AC/DC Hybrid Multi-microgrids, "Bi level two stage Robust Optimal Scheduling," IEEE Transactions on Smart Grid, Early Access, 2018. [3] Haifeng Qiu, et al. [4]

Simulation results with NeuralNetworkController:

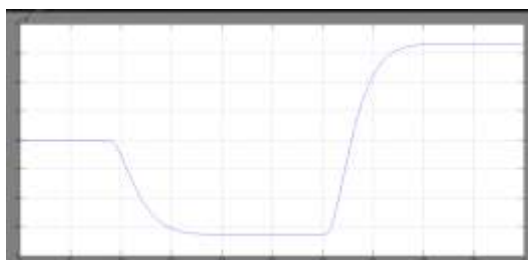


"A Distributed Control Architecture for Global System Economic Operation in Autonomous Hybrid AC/DC Microgrids," by Pengfeng Lin et al., IEE Transactions on Smart Grid, Early Access (2018)

IEEE Transactions on Smart Grid, Vol. 7, No. 1, 2016, pp. 3–5, on decentralized hierarchical control and self-optimizing control techniques for F-P type DGs in islanded microgrids.

This contains Rashmi Pardhi (Priyank Srivastava) and "Power System Stability, FACT Devices, and FACT Device Applications" Journal of Engineering Science

Accessed in: Research and Applications, 2013, Volume



can be c
<http://www.iapb.com>

3, Issue 3, Pages 879-883.

Akanksha Mishra and G.V. Nagesh Kumar's "Interline Power Flow Controller Using Disparity Line for Congestion Management of Power System"

Energy Systems, Volume 1, Issue 3, Pages 76-77.

- In 2015, he was 85 years old.

The stability of the system may be improved by using ABC and GSA algorithms to optimize the location and capacity of UPFCs.

The PECE Conference in Illinois in 2015

K.K. Sen "SSSC-static synchronous series compensator: theory, modeling, and application" appeared in IEEE Transactions on Power Delivery, Volume 13, Number 1, pp. 241–246 in 1998.

UIPC Modeling and Comparison with IPC and UIPFC, J. Pourhossein, et al., IEEE, 2014

biographical information about the author:

Shaik.KALESHA is now being accepted into Quba College of Engineering and Technology's Post-Graduate Program.

Venkatachalam is a city in Nellore. A.P

You may reach me at dsfkn.3ek228@gmail.com.

Graduate degree from Sri Sai Institute Of Technology And Engineering, P.RameshivedSciences Rayachoti, Kadapa, and Quba College Of Engineering And Technology Venkatachalam, Nellore, A.P., where he received a bachelor's degree in electrical and electronics engineering and a master's degree in electrical power systems.